

## Structural and Electrical Properties of Gallium Doped Zinc Oxide Films

Pung Keun Song, Yuzo Shigesato\*, Mika Oguchi\*, Masayuki Kamei and Itaru Yasui

IIS, Uni. of Tokyo, Roppongi, Minato-ku, Tokyo 106-8588, Japan  
\*College of Sci. and Eng., Aoyama Gakuin Uni., Tokyo 157-8572, Japan  
(Received September 23, 1998)

Gallium doped zinc oxide (GZO) films were deposited on soda-lime glass substrates without substrate heating ( $T_s < 50^\circ\text{C}$ ) by dc planar magnetron sputtering using GZO ceramic oxide target with different inert gas (Ar, or Ne). For the GZO films deposited under different total gas pressure ( $P_{\text{tot}}$ ), structural and electrical properties were investigated by XRD and Hall effect measurements. Crystallinity of GZO films deposited using Ar was degraded with increase in  $P_{\text{tot}}$ , suggesting that it was heavily affected by kinetic energy of sputtered Zn particles ( $PA_{\text{Zn}}$ ) arriving at substrate surface. Whereas, crystallinity of GZO films deposited at lower  $P_{\text{tot}}$  than 3.0 Pa using Ne gas was degraded with decrease in  $P_{\text{tot}}$ . This degradation was considered to be result of film damage caused by the bombardment of high-energy neutrals (Ne<sup>0</sup>). On the basis of a hard sphere collision processes, the average final energy of particles (sputtered Zn, Ar<sup>+</sup> and Ne<sup>0</sup>) arriving at substrate surface were estimated.

**Key words:** GZO, DC Magnetron Sputtering, Crystallinity and Electrical Properties, High Energy Particles

### I. Introduction

Non-doped (stoichiometric) ZnO films usually have high resistivity due to the low electron density in the film. Whereas, impurity doped ZnO films showed high conductivity and optical properties. These properties have led to applications of ZnO films as transparent conductors,<sup>1)</sup> transparent window insulation,<sup>2)</sup> gas sensor.<sup>3)</sup> In recent, transparent conducting films based on zinc oxide (ZnO) have been promoted as a promising alternative materials to indium tin oxide (ITO) and tin oxide (SnO<sub>2</sub>) films because of their advantages of low cost, abundant elements, nontoxicity.<sup>4)</sup> It is also reported that ZnO based films are more stable than SnO<sub>2</sub>- and In<sub>2</sub>O<sub>3</sub>-based films in the presence of a hydrogen plasma.<sup>5)</sup> In general, ZnO based films have been prepared by metalorganic chemical vapor deposition,<sup>6)</sup> laser ablation,<sup>7)</sup> magnetron sputtering,<sup>8)</sup> evaporation,<sup>9)</sup> etc. Among these deposition methods, in the case of aluminum, m, and indium doped ZnO films, magnetron sputtering has been frequently used with the deposition of homogeneous large-area films.<sup>4,8,10)</sup> For this sputtering deposition, a few authors reported that high energy particles were generated during the deposition, which affected on the structural and electrical properties of sputtered films. Brodie et al.<sup>11)</sup> observed high-energy neutral atoms (Ar<sup>0</sup>) bombarding the substrate in the sputtering of metal targets such as Cu, W, and Ta. Tominaga et al.<sup>12)</sup> reported the production mechanism of high-energy negative ions (O<sup>-</sup>) and their energy distribution. In the case of ITO, a low resistivity poly-crystalline film was fabricated by improvement of crystallinity, which was achieved by reducing the structural damage due to bom-

bardment of high-energy particles during deposition.<sup>13)</sup> On the other hand, it was also reported that the crystallographic characteristic of ZnO film strongly depended on the sputtering condition or location of substrate.<sup>12)</sup>

As we have mentioned before, Ga-doped ZnO (GZO) films deposited by magnetron sputtering have potential application for conductive transparent electrodes, so it is important to investigate the influence of deposition condition on electrical and structural properties. In this paper, therefore, the effect of  $P_{\text{tot}}$  on structural and electrical properties of GZO film deposited at low substrate temperature ( $T_s$ ) was studied, in connection with estimated kinetic energy of  $PA_{\text{Zn}}$  and high-energy particles (Ar<sup>0</sup>, Ne<sup>0</sup>) which arriving at the substrate surface.

### II. Experimental

GZO films were deposited on soda lime glass substrate by dc planar magnetron sputtering. Oxide ceramic GZO target (doped with 5.7 wt% Ga<sub>2</sub>O<sub>3</sub>, packing density: more than 90%) was used. The films with thickness of 150–200 nm were deposited under different  $P_{\text{tot}}$  using Ar or Ne sputtering gases. Deposition times were adjusted to get a similar film thickness for each deposition condition. These films were deposited at discharge power of 100 W, without substrate heating, where the substrate temperature was measured to be below 50°C using TEMP-PLATE during deposition. Partial pressure of water in the residual gas was controlled lower than 10<sup>-3</sup> Pa using a quadrupole mass spectrometer (MSQ-400, ULVAC) in order to guarantee high reproducibility of films. Room temperature electrical properties (resistivity, carrier density and Hall

mobility) were determined by the 4-point probe method and Hall-effect measurement (Hall System, Bio-Rad). The film thicknesses were measured by a Dektak 3 surface profiler (VEECO/Sloan Tech.). The microstructure of the films was investigated by X-ray diffraction (XRD) with 40 kV-20 mA CuK $\alpha$  radiation (Rigaku, Rint 2000). The crystallite size was determined by Scherrer method,<sup>14</sup> and the measurements were carried out with the step scan mode and a step interval of 0.01°.

### III. Results and Discussion

Figure 1 shows the XRD profiles of the GZO films deposited without substrate heating using only Ar gas at several  $P_{tot}$  (0.25–4.0 Pa) and target-substrate distance ( $T-S$ )=130 mm. The crystallinity of the GZO films was degraded with increase in  $P_{tot}$ . For this degradation in crystallinity, it is considered that crystallinity of GZO films was strongly affected by the kinetic energy of sputtered Zn particles ( $PA_{Zn}$ ) arriving at substrate surface.<sup>15</sup> Based on the assumption that the collision of  $PA_{Zn}$  with the gas molecules is a hard sphere collision process, the kinetic energy ( $E_{Zn}$ ) of  $PA_{Zn}$  arriving at substrate surface can be estimated as follow.<sup>16</sup>

$$E_{Zn} = (E_0 - k_B T_G) \exp \left[ n \ln \left( \frac{E_i}{E_f} \right) \right] + k_B T_G \quad (1)$$

Where,  $E_0$  initial energy of  $PA_{Zn}$  (this was assumed to be 3 eV),  $T_G$  temperature of sputtering gas.  $E_f/E_i$  the ratio of energies before and after a collision, and  $n$  collision number between  $PA_{Zn}$  and gas molecules.  $n$  and  $E_f/E_i$  are given by

$$n = d P_{tot} \sigma / k_B T_G \quad (2)$$

$$E_f/E_i = 1 - \frac{2(m_A m_{Zn})}{(1 + m_A/m_{Zn})^2} \quad (3)$$

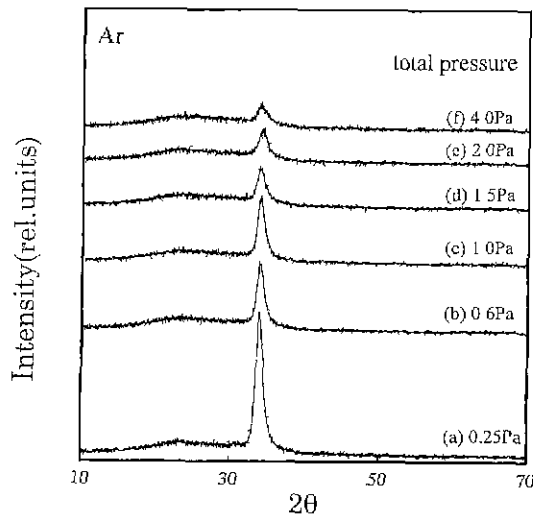


Fig. 1. XRD profiles of GZO films deposited under several total gas pressure using Ar gas only at  $T_s$  below 50°C and target-substrate distance ( $T-S$ )= 130 mm.

**Table 1.** The Variation in Discharge Voltage ( $V_d$ ) and Estimated Average Kinetic Energy of Particles Arriving at Substrate Surface During the Deposition for the GZO Films Deposited Using Ar Gas Under Different  $P_{tot}$  and  $T-S$  of 130 mm at Discharge Power of 100 W.  $E_{Zn}$ : Final Energy of Sputtered Zn Particles,  $E_{Ar^0}$ ,  $E_{PA^0}$ : Initial and Final Energy of Reflected Ar Neutrals,  $E_{IO^-}$ ,  $E_{FO^-}$ : Initial and Final Energy of Negative Oxygen Ions.

$P_{tot}$ (Pa)	$V_d$ (V)	$E_{Zn}$ (eV)	$E_{Ar^0}$ (eV)	$E_{PA^0}$ (eV)	$E_{IO^-}$ (eV)	$E_{FO^-}$ (eV)
0.25	507	1.45	28.7	23.3	507	498
0.6	462	0.48	26.2	17.3	462	441
1.0	426	0.20	24.2	12.1	426	394
2.0	399	0.06	22.6	5.7	399	340
3.0	375	0.05	21.9	2.8	375	270

where  $d$  is the distance traveled,  $\sigma$ : the collision cross section assuming a hard core interaction,  $m_{Zn}$ ,  $m_{Ar}$ : the atomic mass of Zn and Ar. The estimated  $E_{Zn}$  as a function of  $P_{tot}$  are shown in Table 1. The estimated  $E_{Zn}$  decreased with increase in  $P_{tot}$  due to increase in collision number between  $PA_{Zn}$  and Ar gas atoms. From this result, degradation in crystallinity of GZO film with increase in  $P_{tot}$  could be due to decrease in  $E_{Zn}$ , i.e.,  $PA_{Zn}$  were not energetic enough to form the crystalline structure as they arrived at the film surface.

Figure 2 shows the XRD profiles of GZO films deposited using only Ne gas at several  $P_{tot}$  in the same deposition condition as Ar gas. Variation in crystallinity of film with decrease in  $P_{tot}$  showed two patterns, i.e., crystallinity of films was improved with decrease in  $P_{tot}$  until 4.0 Pa, whereas it was degraded again with further decrease in  $P_{tot}$  lower than 4.0 Pa. Two possible effects could be considered for these results. First, improvement in crystallinity with decrease in  $P_{tot}$  until 4.0 Pa can be explained in the same manner as Ar deposition, that is, it

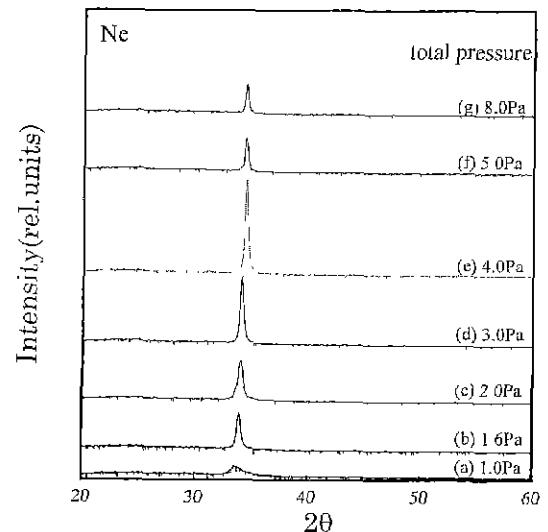


Fig. 2. XRD profiles of GZO films deposited using Ne gas only under different total gas pressure at  $T_s$  below 50°C and  $T-S$ = 130 mm.

might be due to increase in  $E_{Zn}$  of  $PA_{Zn}$  arriving at film surface with decrease in  $P_{tot}$ . One more effect is that the crystallinity of GZO films deposited using Ne gas was affected heavily by the high-energy particles. In general, sputtering process causes energetic particle bombardment on the growing film. The energetic reflected Ar neutrals ( $Ar^0$ ) and the negative oxygen ions ( $O^-$ ) are considered generally as high-energy particles. This  $O^-$  are generated at the target surface, and then accelerated by the cathode potential almost normal to the target surface, and collide with the substrate and induce damages in films. Cuomo *et al.*<sup>17)</sup> suggested that negative ions are predicted by the value of the ionization potential and electron affinity (I-EA) for target element. In particular, Cuomo's model predicts negative ion formation in the case of I-EA lower than 3.4 eV. Ishibashi *et al.*<sup>18)</sup> reported the amount of  $O^-$  flux for YBCO (I-EA=3.75), ITO (I-EA=4.33), ZnO (I-EA=7.93), and BCO (I-EA=3.75) targets in dc sputtering. They also found that the flux of  $O^-$  in ZnO target was less than  $10^{-2}$  of those in YBCO and BCO targets, in good agreement with the Cuomo's model. The initial kinetic energy of  $O^-$  ( $E_{IO^-}$ ) on deposition using Ar or Ne gases are shown in Tables 1 and 2 as a function of  $P_{tot}$ . Each  $E_{IO^-}$  reveals kinetic energy corresponding to the discharge voltage because they were accelerated by cathode potential. If film damage due to  $O^-$  bombardment is present on sputtered GZO films, degradation in crystallinity of film will be observed for the film deposited at low  $P_{tot}$  because  $E_{IO^-}$  (507 eV at 0.25 Pa) for Ar is higher than  $E_{IO^-}$  (299 eV at 1.0 Pa) for Ne. In practice, however, degradation in crystallinity of GZO film deposited using Ar was not observed at even low  $P_{tot}$ . Thus, it can be said that the crystallinity of GZO films deposited using Ar was not strongly affected by the bombardment of  $O^-$ .<sup>19,20)</sup>

On the other hand,  $Ar^0$  are produced by the Auger neutralization and reflection of energetic incident Ar ions at the target surface.<sup>11)</sup> these reflected  $Ar^0$  can have a large fraction of the incident ion energy and may induce significant changes in the structural and electrical properties of the deposited films. In practice, entrapped  $Ar^0$  in metal

films deposited using dc magnetron sputtering were observed,<sup>21)</sup> where the content of them in the films depended on Ar gas pressure, the atomic mass ratio of target and Ar gas, and discharge voltage. In this study, therefore, on the basis of Cuomo's model, we would like to focus on the effect of reflected neutral bombardment on growing films.

Based on a hard sphere collision, initial kinetic energy of high energy Ar neutrals ( $E_{IAr^0}$ ) at 180° reflection (normal to substrate surface) can be estimated as follow,<sup>22)</sup>

$$E_{IAr^0} = \frac{(m_{Zn} - m_{Ar})^2}{(m_{Zn} + m_{Ar})^2} V_c^2 \quad (4)$$

The variation in  $V_c$  of dc sputtering processing using GZO oxide target are shown in Table I as a function of  $P_{tot}$  under the constant discharge power of 100 W. The  $V_c$  decreased due to the increase in discharge current ( $I_c$ ) with increase  $P_{tot}$ , i.e., plasma impedance decreased with increase in  $P_{tot}$ . The values of the estimated initial energy ( $E_{IAr^0}$ ) and final energy ( $E_{FAr^0}$ ) of  $Ar^0$  for each  $P_{tot}$  are shown in Table 1.  $E_{FAr^0}$  were calculated by the equation (1) and (4). In the case of Ne gas, the values of the estimated initial energy ( $E_{INe^0}$ ) and final energy ( $E_{FNe^0}$ ) of  $Ne^0$  are shown in Table 2. In spite of the same discharge power (100 W) and  $P_{tot}$  (1.0 Pa),  $V_c$  in sputtering using Ar showed larger value (426 V) than that of Ne (299 V). This result might be interpreted in terms of the difference in a secondary electron emission rate ( $\gamma_i$ ) which was reported by Hägstrum *et al.*<sup>23)</sup> They reported that  $\gamma_i$  for Ar was much lower than the one for Ne, where the magnitude of the  $\gamma_i$  plays an important role in determining the I-V characteristics of the discharge. In the case of low  $\gamma_i$ , the increase in plasma impedance was considered to be the result of the decrease in number of electrons colliding with gas molecules.<sup>15)</sup>

In the case of Ar, in spite of higher  $V_c$  compared to Ne, estimated  $E_{IAr^0}$  was lower than  $E_{INe^0}$ . This result could be explained in terms of the ratio of energy transfer as two bodies collide. Energy transfer function ( $\gamma$ ) is given by  $\gamma = 4m_{sg}m_{sp} / (m_{sg} + m_{sp})^2$ , where  $m_{sp}$ ,  $m_{sg}$  represent mass of sputter gas ion and target atom, and it increases in case that  $m_{sp}$  is close to  $m_{sg}$ .<sup>24)</sup> Thus,  $\gamma$  of Ar atom colliding with target Zn atom is obviously larger than that of Ne atom because atomic mass of Ar (40 g) is close to Zn (65 g) compare to Ne (20 g). This means that  $Ar^0$  have smaller energy than  $Ne^0$  and it is attributed to the larger energy transferred from Ar atom to Zn atom after collision with target Zn atom. The estimated final energy of reflected neutrals ( $Ar^0$ ,  $Ne^0$ ) decreased with increasing  $P_{tot}$  due to the increase in energy loss caused by the increase in collision number with gas atoms. In the case of Ar,  $E_{FAr^0}$  was estimated to be 23.3 eV at 1.0 Pa. Kubota *et al.*<sup>25)</sup> reported that the crystallinity of film was enhanced by ion energy of 40 eV from the observation for the effect of Ar ion bombardment on crystallographic property of sputtered ITO film. Whereas, in the case of higher energy than 50 eV,

**Table 2.** The Variation in Discharge Voltage ( $V_c$ ) and Estimated Average Kinetic Energy of Particles Arriving at Substrate Surface During Deposition for the GZO Films Deposited Using Ne Gas Under Different Total Gas Pressure ( $P_{tot}$ ) at Distance between Target and Substrate ( $T-S$ ) of 130 mm and Sputtering Power of 100 w.  $E_{Zn}$ : Final Energy of Sputtered Zn Particles,  $E_{INe^0}$ ,  $E_{FNe^0}$ : Initial and Final Energy of Reflected Ne Neutrals ( $Ne^0$ ),  $E_{IO^-}$ ,  $E_{FO^-}$ : Initial and Final Energy of Negative Oxygen Ions.

$P_{tot}$ (Pa)	$V_c$ (eV)	$E_{Zn}$ (eV)	$E_{INe^0}$ (eV)	$E_{FNe^0}$ (eV)	$E_{IO^-}$ (eV)	$E_{FO^-}$ (eV)
1	299	0.63	84	66	299	272
2	267	0.16	75	47	267	218
3	242	0.07	68	25	242	178
4	220	0.05	62	21	220	145
5	207	0.048	58	14	207	122

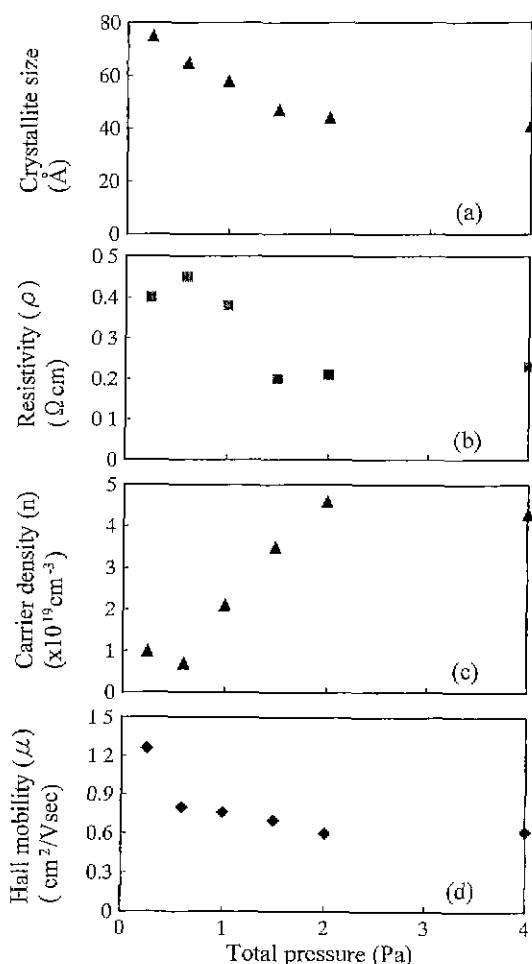


**Fig. 3.** Variation in (a) crystallite size, (b) resistivity, (c) carrier density and (d) Hall mobility of GZO films deposited using Ar gas only under different total gas pressure at  $T_s$  below 50°C

they found that the crystallinity of ITO film was degraded due to film damage caused by ion bombardment. Therefore, it is considered that crystallinity of GZO film deposited using Ar gas was more strongly affected by  $E_{\text{Zn}}$  than  $E_{\text{FAr}}$ , because  $E_{\text{FAr}}$  of 23.3 eV was not energetic enough to cause film damage. On the other hand, in the case of Ne,  $E_{\text{FNe}}$  at 1.0 Pa was estimated to be 66 eV. This energy is considered energetically sufficient to cause structural damage of film from the report of Kubota *et al.*<sup>21)</sup> Thus, degradation in crystallinity of GZO film deposited at 1.0 Pa might be due to film damage caused by bombardment of Ne<sup>+</sup>.

Figure 3 shows crystallite size, resistivity ( $\sigma$ ), carrier density ( $n$ ) and Hall mobility ( $\mu$ ) in GZO films deposited using Ar gas under different  $P_{\text{tot}}$ . With increasing the  $P_{\text{tot}}$ , in spite of degradation in crystallinity of film,  $\sigma$  decreased slightly due to increase in  $n$  whereas  $\sigma$  decreased. The decrease in crystallite size with increase in  $P_{\text{tot}}$  could be interpreted with the increase in nucleation density caused by the generation of inhomogeneous nucleation sites. In general, in the case of transparent conducting films based-

ZnO, carriers are generated by the oxygen vacancy, substitutional atoms and interstitial Zn atoms. In this study,  $n$  showed very small values for GZO films deposited at without substrate heating and relatively larger  $T_s$ . Thus, it is considered that dopant Ga atoms were not activated in GZO film deposited at without substrate heating. Therefore, the increase in  $n$  with increasing  $P_{\text{tot}}$  might be attributed to the increase in interstitial Zn atoms than substitutional Ga atoms.

#### IV. Conclusions

The crystallinity of GZO films deposited without substrate heating was strongly affected by the kinetic energy of particles (sputtered Zn atoms, high energy neutrals) arriving at substrate surface. Based a hard sphere collision model, the kinetic energy of these particles Ne<sup>+</sup>, O<sup>+</sup> was estimated by the equation of K. Meyer and J. A. Thornton. Calculated results showed good agreement with experimental results. In the case of Ar gas, crystallinity of films was mainly affected by kinetic energy of sputtered Zn atoms. On the other hand, in the case of Ne gas, crystallinity of films deposited at relatively low  $P_{\text{tot}}$  was degraded by the film damage. From the result of calculation, it can be explained that the degradation in crystallinity of GZO films deposited at low  $P_{\text{tot}}$  using Ne gas was attributed to film damage caused by bombardment of high energy Ne<sup>+</sup>.

In this study, we could not find film damage caused by the bombardment of high energy O<sup>+</sup>. Consequently, it can be said that the degradation in crystallinity of GZO films was dominated by sputtered Zn atoms and reflected high-energy neutrals. GZO films deposited without substrate heating revealed high resistivity due to low carrier density. In the GZO films deposited using Ar gas, in spite of the degradation in crystallinity of films, decrease in resistivity with increasing  $P_{\text{tot}}$  might be attributed to increase in carrier density caused by increase in interstitial Zn atoms.

#### Reference

1. G. A. Hirata, J. McKittrick, T. Cheeks, J. M. Siqueiros, J. A. Diaz, O. Contreras and O. A. Lopez, "Synthesis and Optoelectronic Characterization of Gallium Doped Zinc Oxide Transparent Electrodes," *Thin Solid Films.*, **288**, 29-31 (1996).
2. M. J. Brett, R. W. MaMahon, J. Affinito and R. R. Parsons. "High Rate Planar Magnetron Deposition of Transparent, Conducting and Heat Reflecting Films on Glass and Plastic," *J. Vac. Sci. Technol.*, A1, 352-355(1983).
3. D. J. Leary, J. O. Barnes and A. G. Jordan, "Calculation of Carrier Concentration in Polycrystalline Films as Function of Surface Acceptor State Density: Application for ZnO Gas Sensor," *J. Electrochem. Soc.*, **129**, 1382-1386(1982).
4. Z.-C. Jin, I. Hamberg and C. G. Granqvist, "Optical Properties of Sputter-deposited ZnO:Al Thin Films," *J. Appl.*

- Phys.*, **64**, 5117-5131(1988).
5. W. M. Duncan, J. W. Lee, R. J. Matyi and H-Y. Liu, "Photoluminescence and X-ray Properties of Heteroepitaxial Gallium Arsenide on Silicon," *J. Appl. Phys.*, **59**, 2161-2164(1986).
  6. W. W. Wenas, A. Yamada, M. Konagami and K Takahashi, "Textured ZnO Thin Films for Solar Cells Grown by Metalorganic Chemical Vapor Deposition," *Jpn. J Appl. Phys*, **30**, L441-443(1991).
  7. G. A. Hirata, J. McKittrick, J. Siqueiros, O. A. Lopez, T. Cheehs, O. Contreras and J. Y. Yi. "High Transmittance-Low Resistivity ZnO:Ga Films by Laser Ablation," *J. Vac. Sci. Technol.* **A14**, 791-794(1996).
  8. R. Wendt and K. Ellmer and K. Wiesemann, "Thermal Power at a Substrate During ZnO:Al Thin Film Deposition in a Planar Magnetron Sputtering System," *J. Appl. Phys.*, **82**, 2115-2122(1997).
  9. H. Sankur and J. T. Cheung, "Highly Oriented ZnO Films Grown by Laser Evaporation," **A1**, 1806-1809(1983)
  10. I. Shih and C. X. Qiu, "Indium-doped Zinc Oxide Thin Films Prepared by RF Magnetron Sputtering," *J. Appl. Phys.*, **58**, 2400-2401(1985).
  11. I. Brodie, L. T. Lamont, Jr. and R. L. Jepsen. "Production of High-energy Neutral Atoms by Scattering of Ions at Solid Surfaces and Its Relation to Sputtering," *Phys. Rev. Lett.*, **21**, 1224-1226 (1968).
  12. K. Tominaga, T. Yuasa, M. Kunc and O. Tada. "Influence of Energetic Oxygen Bombardment on Conductive ZnO Films," *Jpn. J. Appl. Phys.* **24**, 944-949(1985).
  13. Y. Shigesato, S. Takaki and T. Haranoh, "Electrical and Structural Properties of Low Resistivity Tin-doped Indium Oxide Films," *J. Appl. Phys.*, **71**, 3356-3364(1992).
  14. H. P. Klug and L. E. Alexander, "X-ray Diffraction Procedures for Polycrystalline and Amorphous Material," 2nd Ed. by Chap.9 (Wiley, New York, 1994).
  15. P. K. Song, Y. Shigesato, I. Yasui, C. W. Ow-Yang and D. C. Paine, "Study on Crystallinity of Tin-doped Indium Oxide Films Deposited by DC Magnetron Sputtering," *Jpn. J. Appl. Phys.*, **37**, 1870-1876(1998)
  16. K. Meyer, I. K. Schuller and C. M. Falco, "Thermalization of Sputtered Atoms." *J. Appl. Phys.*, **52**, 5803-5805(1981).
  17. J. J. Cuomo, R. J. Gambio, J. M. E. Harper, J. D. Kuptsis and J. C. Webber, "Significance of Negative Ion Formation in Sputtering and SIMS Analysis," *J. Vac. Sci. Technol.*, **15**, 281-287(1978).
  18. K. Ishibashi, K. Hirata and N. Hosokawa, "Mass Spectrometric Ion Analysis in the Sputtering of Oxide Targets," *J. Vac. Sci. Technol.*, **A10**(4), 1718-1722(1992)
  19. P. K. Song, Y. Shigesato, M. Kamei and I. Yasui, "Electrical and Structural Properties of Tin-Doped Indium Oxide Films Deposited by DC Sputtering at Room Temperature," *Jpn. J. Appl. Phys.*, **38**, 2921-2927(1999)
  20. P. K. Song and Y. Shigesato, "Structural Control of TCO Films," *Jpn. J. Surf. Fin. Soc.*, **50**(9), 770-775 (1999).
  21. W. W. Y. Lee and D. Ohlas, "Argon Entrapment in Metal Films by DC Triode Sputtering," *J. Appl. Phys.*, **46**(4), 1728-1732(1975).
  22. J. A. Thornton and D. W. Hoffman, "The Influence of Discharge Current on the Intrinsic Stress in Mo Films Deposited Using Cylindrical and Planar Magnetron Sputtering Source," *J. Vac. Sci. Technol.*, **A3**(3), 576-579(1984).
  23. H. D. Hagstrum. "Auger Ejection of Electrons from Molybdenum by Noble Gas Ions," *Phys. Rev.*, **104**(3), 672-683 (1956).
  24. B. N. Chapman. "Glow Discharge Processes," (John Wiley and Sons, New York) Chap. 1, (1980).
  25. E. Kubota, Y. Shigesato, M. Igarashi, T. Haranoh and K. Suzuki, "Effects of Magnetic Field Gradient on Crystallographic Properties in Tin-Doped Indium Oxide Films Deposited by Electron Cyclotron Resonance Plasma Sputtering." *Jpn. J. Appl. Phys.*, **33**(9A), 4997-5004(1994).